Available online at www.sciencedirect.com
SCIENCE DIRECT
Journal of Sound and Vibration 265 (2003) 647–661
JOURNAL OF SOUND AND VIBRATION
www.elsevier.com/locate/jsvi

An automatic frequency domain modal parameter estimation algorithm

S. Vanlanduit[a,*], P. Verboven[a], P. Guillaume[a], J. Schoukens[b]

[a] *Department of Vibration and Acoustics, Vrije Universiteit Brussel, Pleinlaan 2, B-1050 Brussels, Belgium*
[b] *Department of Fundamental Electricity, Vrije Universiteit Brussel, Pleinlaan 2, B-1050 Brussels, Belgium*

Received 26 April 2002; accepted 29 July 2002

Abstract

In this article, a frequency-domain modal parameter estimation method is proposed. The algorithm automatically separates physical poles from mathematical ones. An important issue in the automatization of the algorithm is the inclusion of noise information to estimate the standard deviations of the poles. These standard deviations are used (together with other features) as the inputs of a fuzzy clustering algorithm. The clustering algorithm then classifies the poles into the mathematical and physical ones. The method requires no user interaction, and a parameter is available quantifying the success of the classification.

1. Introduction

During the last decades, a large number of modal parameter estimation algorithms has been proposed—both in the time and the frequency domain. A crucial step in most of these algorithms is the determination of the correct model order to capture the modes present in the frequency range of interest. Often this model order determination is computationally involved, or a large amount of user interaction is required. Other algorithms perform quite well in ideal laboratory conditions, but fail when the noise level on the measurements increases.

For simple structures in an ideal environment, the detection of the physical poles can be done by means of inspection of mode indicating functions, like frequency response functions (FRFs)

*Corresponding author. Tel.: +32-2-629-2805; fax: +32-2-629-2865.
E-mail address: steve.vanlanduit@vub.ac.be (S. Vanlanduit).

0022-460X/03/$ - see front matter
doi:10.1016/S0022-460X(02)01461-X

and complex mode indicator functions [1]. When the modes are closely spaced or highly damped, or the FRFs are noisy, the model order selection using visual inspection can be tedious and results are often user dependent.

In the modal analysis literature different tools were developed to eliminate computational poles. Most of them give an indication based on the mode shape properties. The mode over complexity [2] computes the mode's average shift due to a mass addition, which gives a value close to unity for physical poles. Other mode shape criteria, like the mode phase collinearity [3] and the mean phase deviation [2] evaluate the degree of relationship between real and imaginary part of the mode shapes.

One of the most widespread techniques to detect physical poles is the so-called stabilization diagram, which is constructed by estimating poles with an increasing model order. Ideally, the physical poles should stabilize, while the computational poles are scattered. For high noise levels the stabilization diagrams can be difficult to interpret and give different results depending on the user. Moreover, stabilization diagrams require interaction and therefore they cannot directly be used when an autonomous modal parameter estimation is needed, as is for example the case for periodic inspection of bridges.

To obtain a fully autonomous modal parameter estimation algorithm several approaches which use neural networks [4], fuzzy logic [5], genetic algorithms [6,7] were proposed recently. Unfortunately the computational load for these methods is quite high.

In the framework of system identification literature, a lot of work has been done on model order selection and model validation in general. For the determination of the correct model order, techniques based on rank testing are often used [8,9]. They allow one to determine an approximate (slightly overestimated) model order which has to be reduced further. The actual validation of the reduced model order is traditionally done using different criteria—like Akaike's information criterion [10,11], the maximum description length [12] and the F-test [13]. Alternatively, the maximum likelihood estimator (MLE) cost function can be used to decide if over or under modelling is present [14]. A problem arises when in addition to the measurement noise, non-linearities or systematic errors are present in the FRFs. In the former case the so-called function of dependency (FOD) can be used [15] as a model validation criterium. The FOD is a particular example of the so-called residual whiteness test [16] which can be used in the presence of high noise levels and non-linear distortions.

Although the mentioned model validation criteria can perform well on validating the model, they cannot be used to detect which poles should be rejected if the model is over fitted. For this goal one of the different existing pole–zero cancellation algorithms can be used [9,17,18]. One of the main disadvantages of these algorithms is that a new identification iteration step is necessary after the deletion of a few pole–zero pairs, making the application unapt when a large amount of measurements has to be processed. In Ref. [19] an approach was proposed to eliminate computational poles in different steps without the need to re-estimate the modal parameters each time a pole is eliminated. The different steps are based on different quantifiers which represent a measure of goodness of a certain mode.

In the next section a global model selection procedure will be outlined which uses a set of well-defined measures as inputs for a clustering algorithm to solve the physical/mathematical classification problem. Because the standard deviations on the poles is an important feature for the classification, a maximum likelihood approach is used.

2. Theory

2.1. Overview of the algorithm

The automatic frequency domain modal parameter estimation algorithm consists of the following steps:

(1) Measure the force(s) and responses of the structure. Convert the data to the frequency domain using an Fast Fourier Transform (FFT) and compute the FRFs.
(2) Estimate the modal parameters using a high model order N_p (for instance use $N_p = 60$ modes).
(3) Classify the N_p modes in physical and computational modes using a clustering algorithm.

Since noise information is important in the presented algorithm it is assumed that in step (1) the variance of the FRFs is also available (remark that the variance is easily obtained when using multiple periods of a periodic excitation signal). The high order modal parameter estimation algorithm that is used in step (2) will be described in Section 2.2. In Section 2.3 the classification in step (3) will be explained.

2.2. Modal parameter estimation

The modal parameter estimation algorithm starts from the MLE-like cost function:

$$\kappa(\theta) = \sum_{k=1}^{N_f} \sum_{i=1}^{N_i} \sum_{o=1}^{N_o} \frac{|H_{oi}(\omega_k) - H_{oi}(\omega_k, \theta)|^2}{var(H_{oi}(\omega_k))}, \tag{1}$$

where $H_{oi}(\omega_k)$ is the measured FRF at output o and input i and $H_{oi}(\theta, \omega_k)$ is the FRF modelled using the following common denominator model:

$$H_{oi}(\theta, \omega_k) = \frac{\sum_{j=1}^{N_p} z^{-k} B_{oij}}{\sum_{j=1}^{N_p} z^{-k} A_j} \tag{2}$$

with $z = e^{\omega j T_s}$ and T_s the sample period. The estimated polynomial model coefficients:

$$\theta = (B_{111} \ \cdots \ B_{N_o N_i 1} \ B_{112} \ \cdots \ B_{N_o N_i 2} \ \cdots \ B_{N_o N_i N_p} \ A_1 \ A_2 \ \cdots \ A_{N_p}) \tag{3}$$

are computed by minimizing Eq. (1). A particular efficient optimization method to perform this task is the well-known Gauss–Newton algorithm (Remark that the cost function (1) has many local minima, so a good choice of starting value estimators like the algorithms presented in Ref. [20] is necessary). After the polynomial coefficients are calculated, the zeros and poles of the system can be computed by calculating the eigenvalues of companion matrices. Finally, the poles p_i and zeros q_i are converted to resonance frequencies $\omega_i = \mathrm{Im}(p_i)$, damping values $\xi_i = \frac{-\mathrm{Re}(p_i)}{\mathrm{Abs}(p_i)}$ and mode shapes Ψ_i.

In Ref. [21] it was shown that by applying structured numerical algorithms, the computation speed of the above-mentioned MLE-like algorithm can be reduced such that the computational load of one iteration of the MLE algorithm is comparable to the well-known least-squares complex exponential (LSCE) [2] algorithm.

Moreover because noise information is used in the estimator, uncertainties on the poles can be computed, practically without additional effort. This noise information is one of the key issues in the success of the model order selection procedure developed in the next section. Further information on the MLE-like modal parameter estimation algorithm can be found in Ref. [21].

2.3. Model order selection by classification

The proposed model order selection consists of the following steps:

(1) Compute and validate a model with a high model order.
(2) Classify modes into physical and computational ones.
(3) Re-iterate the modal parameter estimation process with physical modes only.
(4) Validate the final modal fit.

Steps (1) and (4) can be performed using one of the validation criteria presented above (for example the FOD).

The actual classification in step (2) is done in three stages:

(1) variable selection,
(2) interval scaling,
(3) clustering algorithm.

In the variable selection phase, the criteria which are used to quantify if a pole is physical or not are determined. Using the statistical classification terminology [22], the variables X_k consist of N_p objects, with N_p the number of identified modes (both computational and physical). The goal is to use as much of the available information (of the estimated poles and mode shapes) without significantly increasing the computational load of the identification procedure. The following eight criteria serve this goal:

(1) *Variable 1*: X_1 are the standard deviations of the estimated resonance frequencies (computed in the MLE).
(2) *Variable 2*: X_2 are the standard deviations of the estimated damping values.
(3) *Variable 3*: X_3 are the standard deviations of the estimated damping values over the last half of the MLE Newton–Gauss.
(4) *Variable 4*: X_4 are the standard deviations of the estimated resonance frequencies over the last half of the MLE Newton–Gauss.
(5) *Variable 5*: X_5 gives an indication of the stabilization of the pole with an increasing model order. The criterion gives a quantitative value to the amount in which a maximal order pole stabilizes in the MLE stabilization diagram by computing the standard deviation with respect to poles at lower model orders. (To pair poles of two different model orders, the closest poles are chosen, unless the distance between two poles is larger than, e.g., three times the standard deviation. In the latter case the pole is considered to become unstable at that order. In this case no pairing pole is used.) To give early stabilizing poles a higher weight, the standard deviation is multiplied with the lowest order at which it is still stable (i.e., changes smaller than three times the standard deviation).

(6) *Variable 6*: X_6 is the number of sign changes in each of the mode shapes to detect if the mode shapes are spatially correlated:

$$X_6(r) = \#\{i \mid \Psi_r(x_i, y_i).\Psi_r(x_{i+1}, y_{i+1}) < 0\}$$

with Ψ_r the rth mode shape and x_i and y_i represent the spatial co-ordinates of the vibration pattern outputs, with i for instance the ranking number of the output obtained by sorting the magnitudes of the x and y co-ordinates (alternatively, if the sorting of the d.o.f.s is not possible, the MPC or MPD can also be used for Variable 6.)

(7) *Variable 7*: X_7 is the number of zeros which fall in $3\sigma_{p_r}$ uncertainty sphere around each pole p_r ($\sigma_{p_r} = std(p_r)$ is the uncertainty on pole number r, for $r = 1, \ldots, N_p$). (Remark that because physical poles are usually well separated by the zeros, the variable also works when instead of three the uncertainty sphere is more than three (e.g., 10) times larger than σ_{p_r}.)

(8) *Variable 8*: X_8 is the inverse of the root mean squared (RMS) magnitude of the mode shape Ψ_r for $r = 1, \ldots, N_p$.

The selection of the criteria is based on the observation that estimated poles which model the noise in the measurements:

- Have a large uncertainty (Variables 1 and 2).
- Converge slower (Variables 3 and 4).
- Do not stabilize with an increasing model order (Variable 5).
- Give rise to noisy mode shapes (Variable 6).
- Usually have a number of cancelling zeros in their neighborhood (Variable 7).
- Lead to small magnitude mode shapes.

The computational load for the variable selection step is negligible (typically a few seconds) compared to the modal parameter estimation step. After the variables have been computed, an interval scaling [22] is performed in order to obtain variables of the same type, which are defined in the same interval (e.g., [0, 1]). In a first step of the interval scaling procedure, the variables with a large range (i.e., all variables except X_6 and X_7) are transformed using a logarithmic transform (Without this transform outliers which could give rise to an erroneous classification could be present.) Secondly, all variables are subtracted by their minimum and divided by their range (i.e., the maximum minus minimum).

The actual clustering algorithm determines the success of the classification of the objects. An iterative fuzzy C-means clustering algorithm [23], implemented in the Matlab fuzzy logic toolbox [24], was used. The algorithm works as follows:

(1) INITIALIZATION STEP
Select random cluster centres c_j^k (j denotes the Variable and k the cluster number).
Compute the distance d_{ik} from the objects x_{ij} to the centres c_j^k:

$$d_{ik}^2 = \sum_{j=1}^{J} (x_{ij} - c_j^k)^2. \quad (4)$$

For each object x_i compute the membership function μ_{ik} with respect to cluster k:

$$\mu_{ik}^2 = \sum_{l=1}^{K} \left(\frac{d_{ik}}{d_{il}} \right)^{2/(m-1)} \tag{5}$$

with m the fuzzy-ness factor (typically $m = 2$).

(2) ITERATION STEPS

FOR $n = 1, \ldots, N_{iter}$

(a) Update the centres c_j^k with respect to cluster k:

$$c_j^k = \frac{\sum_{i=1}^{I} (\mu_{ik})^m x_{ij}}{\sum_{i=1}^{I} \mu_{ik}}. \tag{6}$$

(b) Update the distances d_{ik} in Eq. (4) using the new centres c_j^k.

(c) Update the membership functions μ_{ik} in Eq. (5) using the new distances d_{ik}.

(d) Compute the cost function δ:

$$\delta = \sum_{i=1}^{I} \sum_{k=1}^{K} (\mu_{ik})^m d_{ik}^2 \tag{7}$$

END

The output of the algorithm gives a membership function μ_{ik} for the classes of physical and computational poles (i.e., $K = 2$). If the membership function for an object with respect to a class is larger than 50% then it is decided that the object belongs to that class.

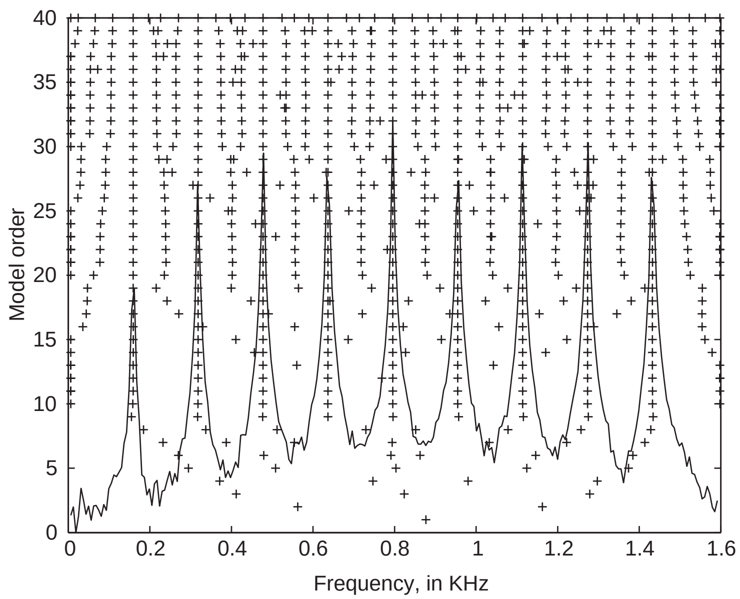

Fig. 1. Stabilization diagram for the simulation data, using the LSCE estimator.

In the following sections it will be shown by means of simulations and experimental data that the classification approach usually gives good results, even if some of the variables do not allow a successful classification.

3. Simulations

An FRF matrix for a system with nine modes (damping values 1%, equidistant resonance frequencies between 0 Hz and 1.6 kHz and mode shapes with consecutive

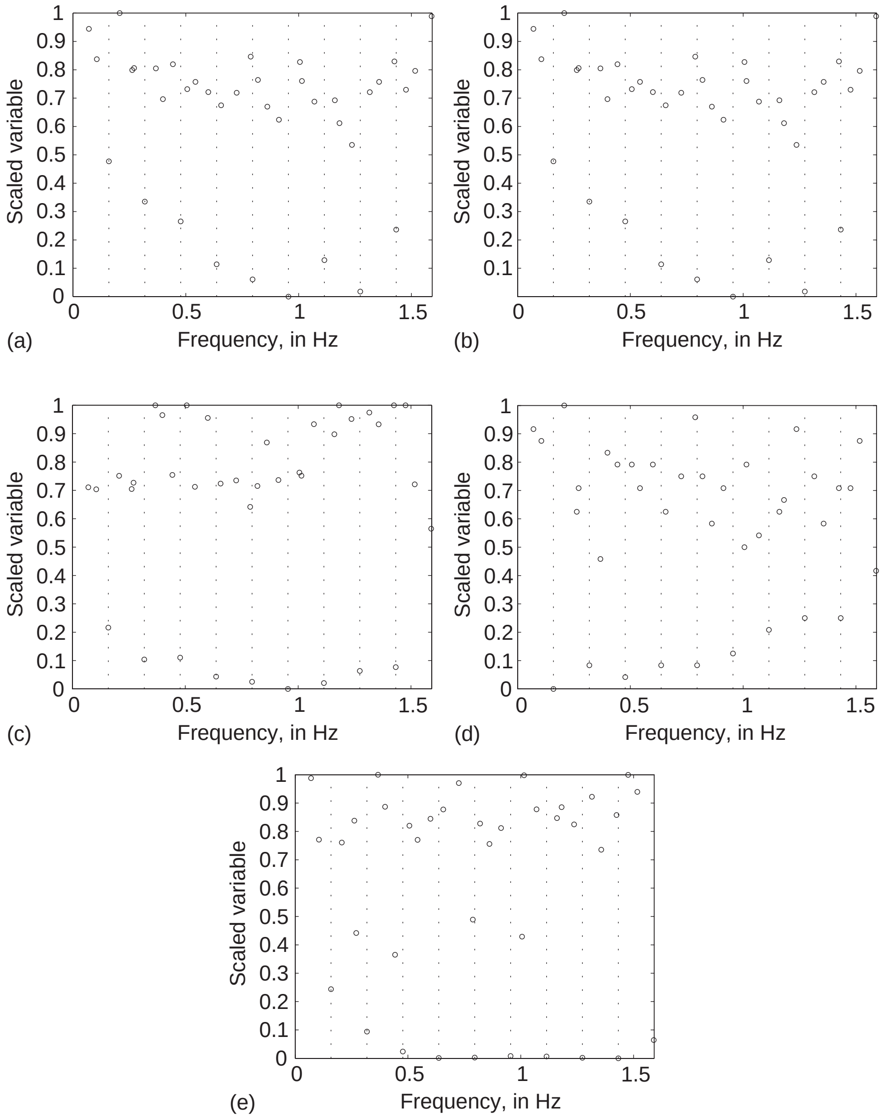

Fig. 2. (a) Variable 2, (b) Variable 3, (c) Variable 5, (d) Variable 6, (e) Variable 8 used to classify the poles for the simulation data. o, estimated poles; ⁝, physical poles.

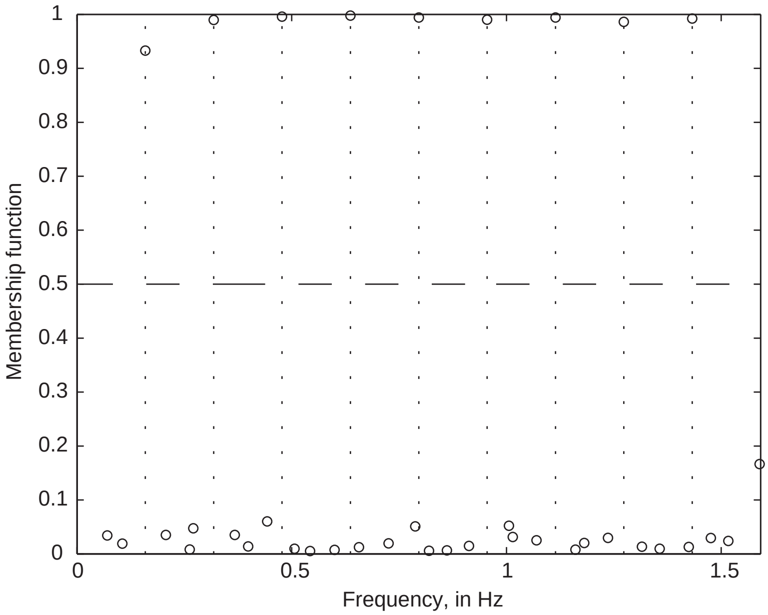

Fig. 3. Classification result for the simulated data. o, estimated poles; ⋮, physical poles; - -, threshold for accepting a physical pole.

wave number sines) was generated at 256 frequencies and 20 outputs. Then, 1% of noise was added.

From Fig. 1, where the LSCE stabilization diagram is shown, it can be seen that besides the true system poles other mathematical poles seem to stabilize. This is caused by the fact that the LSCE fits the noise when a high degree of over-modelling is used. Although the selection of the physical poles from the LSCE stabilization diagram in Fig. 1 would not cause too much problem for an experienced user, the procedure could not be applied autonomously.

When looking at the variables used in the automatic classification approach (Fig. 2), it is clear that is not possible to separate the physical and the mathematical poles by inspecting the variables individually. Indeed, Variable 8 (Fig. 2(e)) has a low value for the mathematical pole around 1.6 kHz, while Variables 2 (Fig. 2(a)) and 3 (Fig. 2(b)) have high values for the first three physical poles. Nevertheless, the classification is performed successfully (see Fig. 3). The true physical poles (indicated by the vertical dotted lines) have a membership degree of more than 90% for the physical pole class and are therefore far above the 50% threshold (dashed horizontal line) used to decide if a pole is a physical or a mathematical one.

4. Experiments

In this section some experimental results of the automatic modal parameter estimation algorithm will be discussed. Firstly, the proposed technique will be illustrated using good quality

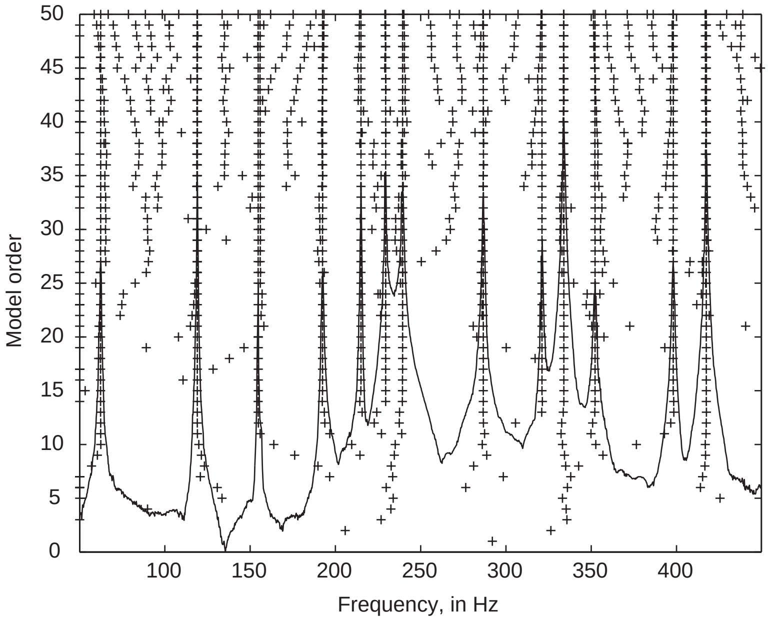

Fig. 4. Stabilization diagram for the sub-frame measurements, using the LSCE estimator.

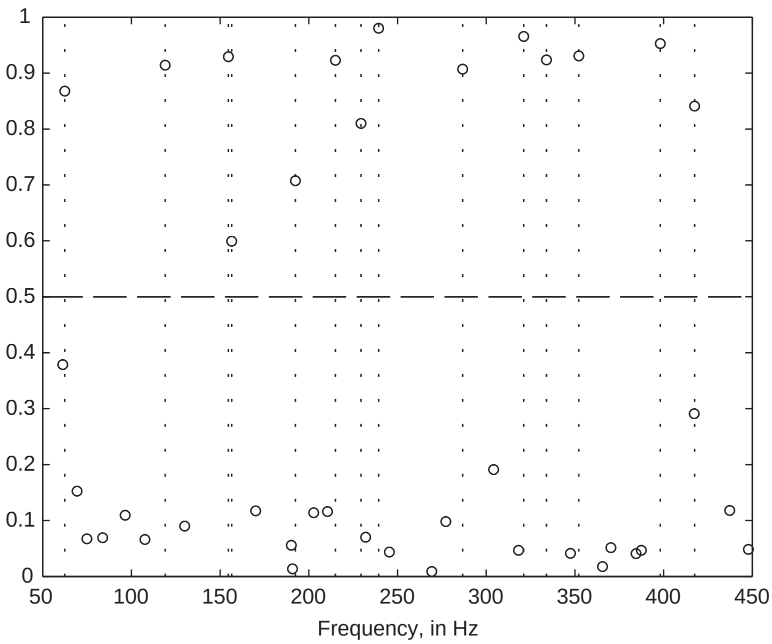

Fig. 5. Classification result for the sub-frame data. o, estimated poles; ⁚, physical poles; - -, threshold for accepting a physical pole.

measurement a car sub-frame (Section 4.1). Secondly, results on poor quality laser vibrometer measurements will be shown (Section 4.2).

4.1. Sub-frame data

The device under test is a structure which is constructed to resemble the sub-frame on which the engine of a car is mounted. Twenty-eight outputs were measured while exciting the structure with uncorrelated white noise sequences at two locations. Measurements were made up to 512 Hz with a frequency resolution of 0.25 Hz. More details on the setup can be found in Ref. [25].

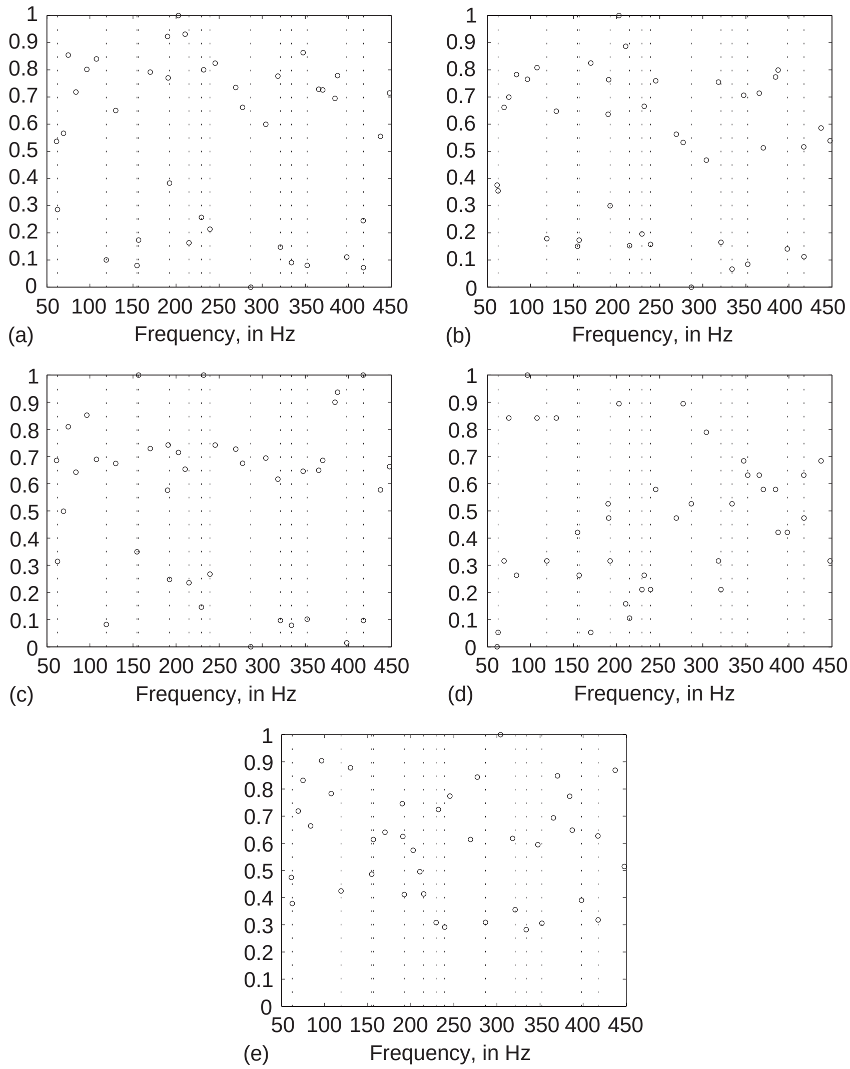

Fig. 6. (a) Variable 2, (b) Variable 3, (c) Variable 5, (d) Variable 6, (e) Variable 8 used to classify the poles for the sub-frame measurements. o, estimated poles; ⁚, physical poles.

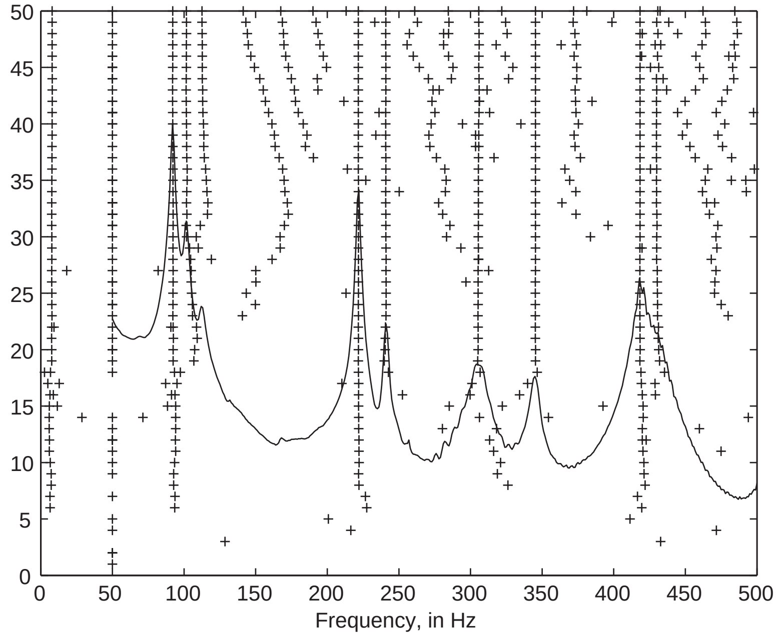

Fig. 7. Stabilization diagram for the composite reference measurements (SNR = 30 dB), using the LSCE estimator.

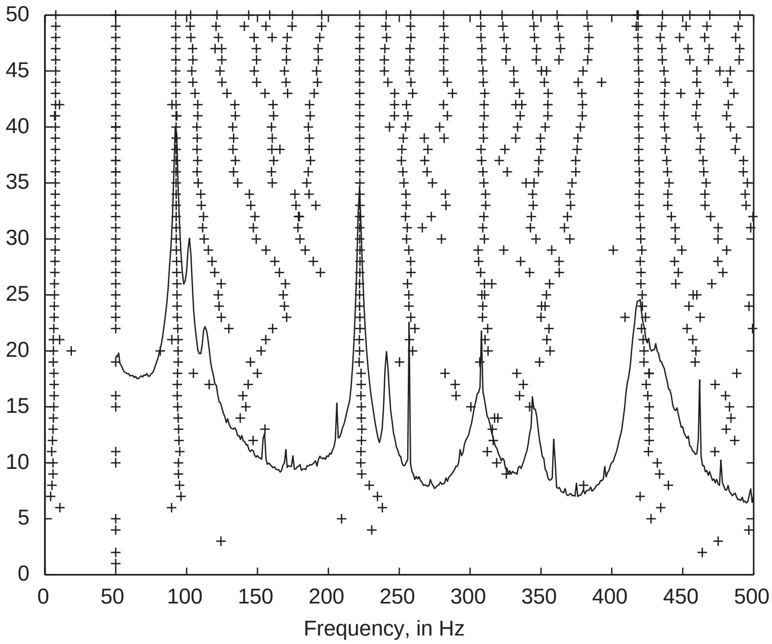

Fig. 8. Stabilization diagram for the poor quality composite measurements (SNR = 0 dB), using the LSCE estimator.

The LSCE stabilization diagram in Fig. 4 is reasonably clear and 14 poles can be selected in the frequency range of interest.

The clustering algorithm is performed with success (see Fig. 5). The pole around 156 Hz however has a reasonably low membership function (60%). This is not surprising, since for some of the variables (used in the classification approach) this pole belongs to the class of the mathematical poles (in particular Variable 5 gives incorrect information as can be seen in Fig. 6). Still, the classification result is quite acceptable.

4.2. Composite data

A composite rectangular panel of 25 cm $\times$ 20 cm with a thickness of about 3 mm was measured with a scanning laser vibrometer at 40 by 30 spatial locations. The panel was excited with a periodic excitation signal and measurements up to 1 kHz were made with a frequency resolution of 1 Hz. Firstly, a reference measurement with a good quality (average signal-to-noise ratio (SNR) about 30 dB) was performed (see the stabilization diagram in Fig. 7). From this reference measurement the modes which were present could be extracted. The actual measurement which was used to validate the model order selection procedure was obtained by reducing the excitation amplitude (and therefore the SNR) with 30 dB. For clarity of the figures only the frequency range up to 500 Hz is displayed.

From the stabilization diagram in Fig. 8 it can be seen that several physical modes cannot be found back anymore. This is the case for modes around 100, 240, 340 and 430 Hz. Moreover, a disturbance due to noise gives rise to a stabilizing behaviour around 260 Hz.

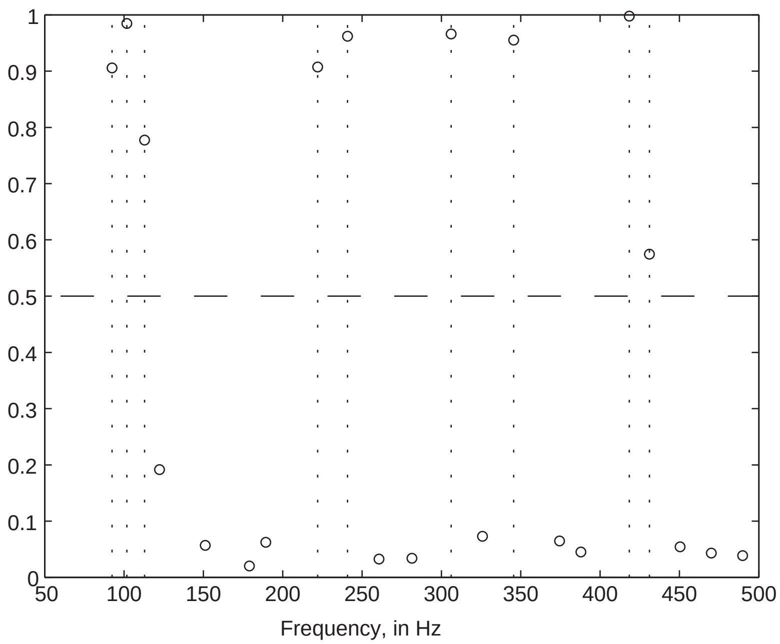

Fig. 9. Classification result for the composite panel measurements. o, estimated poles; $\vdots$, physical poles; - -, threshold for accepting a physical pole.

The proposed automatic modal parameter estimation algorithm, however, enables the detection of all nine modes from the noisy (0 dB SNR) FRFs (see Fig. 9). This is remarkable considering the poor quality of the data, and the failure of some of the variables used in the classification (see Fig. 10).

5. Conclusions

In this paper an automatic modal parameter estimation algorithm, based on the maximum likelihood estimator, was proposed. The standard deviations of the poles were used (together with

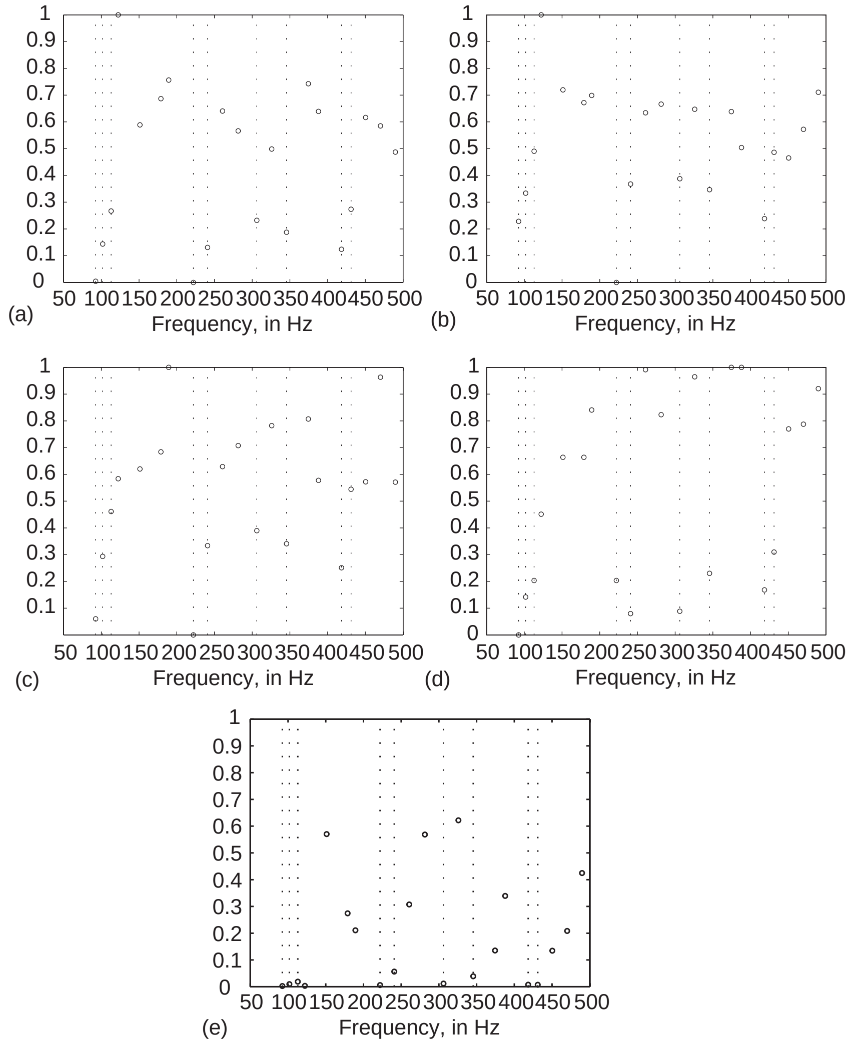

Fig. 10. (a) Variable 2, (b) Variable 3, (c) Variable 5, (d) Variable 6, (e) Variable 8 used to classify the poles for the composite panel measurements. o, estimated poles; ⁝, physical poles.

other quantitative criteria of the poles and the mode shapes) to quantify the degree of 'physicalness' of a mode. By making use of a clustering algorithm, the classification of physical and computational poles could be performed in an automatic manner. Even if some of the criteria (i.e., variables) did not allow a correct classification, the global clustering result was satisfying—even in the case of high noise levels and highly coupled modes.

Acknowledgements

This research has been sponsored by the Flemish Institute for the Improvement of the Scientific and Technological Research in Industry (IWT), the Fund for Scientific Research–Flanders (Belgium) (FWO-Vlaanderen), the Flemish government (GOA-IMMI) and the Belgian government as a part of the Belgian program on Interuniversity Poles of attraction (IUAP50) initiated by the Belgian State, Prime Ministers Office Science Policy Programming. The authors also would like to thank LMS International for providing the measurement data on the subframe.

References

[1] C.Y. Shih, Y.G. Tsuei, R.J. Allemang, D.L. Brown, Complex mode indicator function and its application to spatial domain parameter estimation, Mechanical Systems and Signal Processing 2 (4) (1988) 367–377.
[2] LMS CADA-X, LMS CADA-X User Manual, Modal Analysis, Rev 3.4, LMS International, Leuven, Belgium, 1996.
[3] J.-N. Juang, R.S. Pappa, An eigensystem realization algorithm for modal parameter identification and model reduction, Journal of Guidance, Control and Dynamics 8 (5) (1985) 620–627.
[4] T. Lim, R. Cabell, R. Silcox, On-line identification of modal parameters using artificial neural networks, Journal of Vibration and Acoustics 118 (4) (1996) 649–656.
[5] S. Woodard, R. Pappa, Development of structural identification accuracy indicators using fuzzy logic, in: ASME Design Engineering Technical Conferences, no. DETC97/VIB-4258, Sacramento, CA, 1997.
[6] G.H. James III, D.C. Zimmerman, K.S. Chhipwadia, Application of autonomous modal identification to traditional and ambient data sets, in: Proceedings of the 17th International Modal Analysis Conference, 1999, pp. 840–845.
[7] K.S. Chhipwadia, D.C. Zimmerman, G.H. James III, Evolving autonomous modal parameter estimation, in: Proceedings of the 17th International Modal Analysis Conference, Kissimmee, FL, 1999, pp. 819–825.
[8] C.M. Woodside, Estimation of the order of linear systems, Automatica 7 (1971) 727–733.
[9] Y. Rolain, J. Schoukens, R. Pintelon, Order estimation for linear time-invariant systems using frequency domain identification methods, IEEE Transactions an Automatic Control 42 (10) (1997) 1408–1417.
[10] H. Akaike, A new look at the statistical model identification, IEEE Transactions on Automatic Control AC-19 (1974) 716–723.
[11] H. Akaike, Modern development of statistical methods, in: P. Eykhoff (Ed.), Trends and Progress in System Identification, Pergamon Press, Elmsford, USA, 1981.
[12] J. Rissanen, Prediction minimum description length principles, The Annals of Statistics 14 (1986) 1080–1100.
[13] T. Söderström, On model structure testing in system identification, Automatica 11 (1975) 537–541.
[14] R. Pintelon, P. Guillaume, J. Schoukens, Measurement of noise (cross-) power spectra for frequency-domain system identification purposes: large-sample results, IEEE Transactions on Instrumentation and Measurement 45 (1) (1996) 12–20.
[15] J. Schoukens, T. Dobrowiecki, R. Pintelon, Parametric and non-parametric identification of linear systems in the presence of nonlinear distortions, IEEE Transactions on Automatic Control 43 (2) (1998) 176–191.
[16] L. Ljung, System Identification: Theory for the User, 2nd Edition, Prentice-Hall, Englewood Cliffs, NJ, 1999.

[17] T. Söderström, Tests of pole–zero cancellation in estimated models, Automatica 11 (1975) 537–541.
[18] S. Gyula, J. Schoukens, Y. Rolain, Automatic Model Selection for Linear Time-invariant Systems, Proceedings of the IFAC System Identification Conference, Santa Barbara, USA, 2000.
[19] P. Verboven, E. Parloo, P. Guillaume, M. Van Overmeire, Autonomous modal parameter estimation based on a statistical frequency domain maximum likelihood approach, in: Proceedings of the 19th International Modal Analysis Conference, 2001.
[20] P. Verboven, P. Guillaume, M. Van Overmeire, Modal parameter identification: estimation of starting values for MLE-like algorithms, in: Proceedings of the 23rd International Seminar on Modal Analysis, Leuven, Belgium, 1998.
[21] P. Guillaume, P. Verboven, S. Vanlanduit, Frequency-domain maximum likelihood identification of modal parameters with confidence intervals, in: Proceedings of the 23rd International Seminar on Modal Analysis, Leuven, Belgium, September 1998.
[22] L. Kaufman, P.J. Rousseeuw, Finding Groups in Data, Wiley Series in Probability and Mathematical Statistics, Wiley, New York, 1990.
[23] J.C. Bezdek, Pattern Recognition with Fuzzy Objective Function Algorithms, Plenum Press, New York, 1981.
[24] L.A. Zadeh, Fuzzy Logic Toolbox for Use with MATLAB, The MathWorks Inc., Natick, MA, 1995.
[25] L. Hermans, H. Van der Auweraer, M. Abdelghani, A critical evaluation of modal parameter extraction schemes for output-only data, in: Proceedings of the International Modal Analysis Conference Japan, 1997, pp. 682–688.